

August 2003
 hep-ph/0308254

Implications of the DAMA and CRESST experiments for mirror matter-type dark matter

R. Foot¹

School of Physics,
 University of Melbourne,
 Victoria 3010 Australia

Mirror atoms are expected to be a significant component of the galactic dark matter halo if mirror matter is identified with the non-baryonic dark matter in the Universe. Mirror matter can interact with ordinary matter via gravity and via the photon-mirror photon kinetic mixing interaction { causing mirror charged particles to couple to ordinary photons with effective electric charge e . This means that the nuclei of mirror atoms can elastically scatter off the nuclei of ordinary atoms, leading to nuclear recoils, which can be detected in existing dark matter experiments. We show that the dark matter experiments most sensitive to this type of dark matter candidate (via the nuclear recoil signature) are the DAMA/NaI and CRESST/Sapphire experiments. Furthermore, we show that the impressive annual modulation signal obtained by the DAMA/NaI experiment can be explained by mirror matter-type dark matter for $j \approx 5 \times 10^9$ and is supported by DAMA's absolute rate measurement as well as the CRESST/Sapphire data. This value of j is consistent with the value obtained from various solar system anomalies including the Pioneer spacecraft anomaly, anomalous meteorite events and lack of small craters on the asteroid Eros. It is also consistent with standard BBN.

¹E-mail address: rfoot@unimelb.edu.au

The DAMA/NaI experiment [1, 2] has been searching for dark matter and has obtained some very exciting positive results which merit serious consideration. While they have interpreted their data in terms of weakly interacting heavy particles an alternative interpretation will be suggested here.

In the DAMA/NaI experiment the target consists of 100 kg of radiopure NaI. The aim of the experiment is to measure recoil energy of the Na, I atoms due to interactions of dark matter particles with their detector. Due to the Earth's motion around the sun, the rate should experience a small annual modulation:

$$A \cos 2 (\pi (t - t_0)/T) = T \quad (1)$$

According to the DAMA analysis [2], they indeed find such a modulation over 7 annual cycles at more than 6 C.L. Their data fit gives $T = (1.00 \pm 0.01)$ year and $t_0 = 144 \pm 22$ days, consistent with the expected values. [The expected value for t_0 is 152 days (2 June), where the Earth's velocity, v_E , reaches a maximum with respect to the galaxy]. The strength of their signal is $A = (0.019 \pm 0.003)$ cpd/kg/keV.

The DAMA collaboration have interpreted these impressive results as evidence for heavy weakly interacting dark matter particles. However, another possibility is that this experiment has observed the impacts of galactic mirror atoms, as will shortly be explained.

Mirror matter is predicted to exist if nature exhibits an exact unbroken mirror symmetry [3] (for reviews and more complete set of references, see Ref. [4]). For each type of ordinary particle (electron, quark, photon etc) there is a mirror partner (mirror electron, mirror quark, mirror photon etc), of the same mass. The two sets of particles form parallel sectors each with gauge symmetry G (where $G = SU(3) \times SU(2) \times U(1)$ in the simplest case) so that the full gauge group is $G \times G$. The unbroken mirror symmetry maps $\psi \rightarrow \psi$ as well as ordinary particles into mirror particles. Exact unbroken time reversal symmetry also exists, with standard CPT identified as the product of exact T and exact P [3].

Ordinary and mirror particles can interact with each other by gravity and via the photon-mirror photon kinetic mixing interaction:

$$L = -\frac{F}{2} F^0 \quad (2)$$

where $F = (F^0)$ is the field strength tensor for electromagnetism (mirror electromagnetism)². Photon-mirror photon mixing causes mirror charged particles to couple to ordinary photons with a small effective electric charge, e [3, 7, 8]. Interestingly, the existence of photon-mirror photon kinetic mixing allows mirror matter to explain a number of puzzling observations, including the Pioneer spacecraft anomaly [9, 10], anomalous

² Given the constraints of gauge invariance, renormalizability and mirror symmetry it turns out [3] that the only allowed non-gravitational interactions connecting the ordinary particles with the mirror particles are via photon-mirror photon kinetic mixing and via a Higgs-mirror Higgs quartic interaction, $L = \frac{1}{2} \psi^\dagger \psi \phi^0$. If neutrinos have mass, then ordinary-mirror neutrino oscillations may also occur [5, 6].

meteorite events [11, 12] and the unexpectedly low number of small craters on the asteroid 433 Eros [13, 14]. It turns out that these explanations and other constraints [15, 16] suggest that ρ is in the range

$$10^{-9} < \rho < 5 \times 10^{-7} \text{ g cm}^{-3} \quad (3)$$

More generally, mirror matter is a rather obvious candidate for the non-baryonic dark matter in the Universe because:

It is well motivated from fundamental physics since it is required to exist if parity and time reversal symmetries are exact, unbroken symmetries of nature.

It is necessarily dark and stable. Mirror baryons have the same lifetime as ordinary baryons and couple to mirror photons instead of ordinary photons.

Mirror matter can provide a suitable framework for which to understand the large scale structure of the Universe [17].

Recent observations from WMAP [18] and other experiments suggest that the cosmic abundance of non-baryonic dark matter is of the same order of magnitude as ordinary matter ρ_{dark} . A result which can naturally occur if dark matter is identified with mirror matter [19].

If mirror matter is identified as the non-baryonic dark matter, then the dark matter halo will consist of compact objects such as mirror stars and planets, as well as a mirror gas and dust component. Evidence for mirror stars arises from MACHO observations [20, 21] (and to some extent from the puzzling 'isolated' planets [22]) while the existence of close-in extrasolar planets can also be viewed as mirror matter manifestations [23]. The amount of material in compact form is probably less than 50% (coming from the MACHO upper limit). Thus we expect a dark matter halo with a significant gas/dust component containing mirror H^0 ; He^0 + heavier mirror elements. Assuming a local halo dark matter energy density of 0.3 GeV cm^{-3} , then the number densities of $A^0 = H^0$; He^0 and heavier elements is then given by

$$n_{A^0} = \frac{0.3 \text{ GeV cm}^{-3}}{M_{A^0}} \quad (4)$$

where $\frac{A^0}{A^0} = (0.3 \text{ GeV cm}^{-3})$ is the A^0 proportion (by mass) of the halo dark matter. As discussed above, a plausible value for $\frac{A^0}{A^0}$ is $\frac{1}{2}$.

Arguments from early Universe cosmology (mirror BBN) [17] suggest that He^0 dominates over H^0 , quite unlike the case with ordinary matter. Mirror elements heavier than H^0 ; He^0 will presumably come from nucleosynthesis within mirror stars, qualitatively similar to the ordinary matter case. In the ordinary matter case, the galactic relative (mass) abundance of elements heavier than H ; He (collectively called 'metals' in the astrophysics literature) is estimated [24] to be roughly $Z_{\text{g}} \approx 0.02$ ($\frac{M_{\text{metals}}}{M_{\text{H+He}}} \approx 0.10$). These heavier elements are made up primarily (> 90%) of O, Ne, N, C which have $M_A = M_P \times 16/4$; $Z = 8/2$. Thus, oxygen provides an excellent 'average' for ordinary elements heavier than helium { except perhaps for iron [which is about 10 times

less abundant (by mass) than oxygen]. In the case of minor element abundances, we would expect a qualitatively similar picture, i.e. O^0 (and elements with nearby atomic number) should dominate the energy density after $H^0; H^e$, with a possible small Fe^0 contribution. Thus we need only consider four minor elements: $H^0; H^e; O^0; Fe^0$ (where O^0 stands for Oxygen and nearby elements). Of course, quantitatively, the ratios $O^0 = H^e$; $Fe^0 = O^0$ are quite uncertain because of the different initial values for $H^e = H^0$ (coming from minor BBN) and other different initial conditions. Although the proportion of the various minor elements in the halo (gas/dust ratio etc) is uncertain, the mass scale is not a free parameter: minor hydrogen, H^0 , is predicted to have exactly the same mass as ordinary hydrogen, i.e. $M_{H^0} = 0.94 \text{ GeV}$, minor helium, H^e , has mass $M_{H^e} = 3.76 \text{ GeV}$ etc³.

In an experiment such as DAMA/NaI, the measured quantity is the recoil energy, E_R , of a target atom. The minimum velocity of a minor atom of mass M_{A^0} impacting on a target atom of mass M_A is related to E_R via the kinematic relation:

$$v_{\text{min}} = \frac{v_{\text{cut}}}{\frac{(M_A + M_{A^0})^2 E_R}{2 M_A M_{A^0}}}: \quad (5)$$

Interestingly, most of the existing dark matter experiments are not very sensitive to minor matter-type dark matter because v_{min} [Eq.(5)] turns out to be too high. This is because they either use target elements which are too heavy (i.e. large M_A) or have a E_R threshold which is too high. For example, the CDM S experiment uses Ge as the target material and has a threshold of 10 keV [27]. This means that $v_{\text{min}} \approx 1600 \text{ km/s}$ (for H^e). Although there would be no cutoff velocity at the galactic escape velocity for H^e due to H^e self interactions, the number of H^e with such high velocities would be negligible. The existing experiments with the greatest sensitivity to light minor elements are the DAMA/NaI [1, 2] and the CRESST/sapphire experiments [28]. Both of these experiments will be examined in detail.

When a minor atom (of mass M_{A^0} , atomic number Z^0) encounters ordinary matter (comprised of atoms with mass M_A , atomic number Z) Rutherford scattering can occur, with center of mass cross section:⁴

$$\frac{d\sigma}{d\Omega}_{\text{elastic}} = \frac{Z^2 Z^0 M_{\text{red}}^2}{4 M_{A^0}^4 v_{\text{cm}}^4 \sin^4 \frac{\theta}{2}} F_A^2(qr_A) F_{A^0}^2(qr_{A^0}) \quad (6)$$

where v_{cm} is the center of mass velocity of the impacting minor atom and $M_{\text{red}} = M_A M_{A^0} / (M_A + M_{A^0})$ is the reduced mass⁵. In Eq.(6), $F_X(qr_X)$ ($X = A; A^0$) are the form factors which take into account the finite size of the nuclei and minor nuclei.

³ It is possible to construct minor matter models with broken minor symmetry, in which case the masses of the minor particles need not be the same as their ordinary counterparts [25], but these models tend to be more complicated and/or less well motivated than the simplest case of unbroken minor symmetry [26].

⁴ Note that unless otherwise stated, we use natural units where $\hbar = c = 1$.

⁵ Due to the screening effects of the atomic electrons, the cross section is modified (and becomes suppressed) at small scattering angles [$\theta < 1 = (M_{A^0} v r_0)$ with $r_0 \approx 10^{-9} \text{ cm}$].

($q = (2M_A E_R)^{1/2}$ is the momentum transfer and r_X is the effective nuclear radius). A simple analytic expression for the form factor, which we adopt in our numerical work, is [29]:

$$F_X(qr_X) = 3 \frac{j_1(qr_X)}{qr_X} e^{-(qs)^2/2} \quad (7)$$

with $r_X = 1.14 X^{1/3} \text{ fm}$, $s = 0.9 \text{ fm}$.

This cross section, Eq.(6), can be expressed in terms of the recoil energy of the ordinary atom, E_R , and lab velocity, v (i.e. the velocity in Earth rest frame):

$$\frac{d}{dE_R} = \frac{1}{E_R^2 v^2} \quad (8)$$

where

$$\frac{2^2 Z^2 Z^2 \varnothing}{M_A} F_A^2(qr_A) F_{A^0}^2(qr_{A^0}) \quad (9)$$

Note the $1/E_R^2$ dependence. It arises because the dark matter particles interact electromagnetically (i.e. via exchange of massless photons). This is quite unlike the standard WIMP case and therefore represents a major difference between mirror dark matter and standard WIMP dark matter.

The interaction rate is

$$\begin{aligned} \frac{dR}{dE_R} &= \sum_{A^0} N_T n_{A^0} \int \frac{d}{dE_R} \frac{f(v; v_E)}{k} |\mathbf{v}| d^3v \\ &= \sum_{A^0} N_T n_{A^0} \frac{1}{E_R^2} \int_{v_{\min}(E_R)}^{v_{\max}} \frac{f(v; v_E)}{k |\mathbf{v}|} d^3v \end{aligned} \quad (10)$$

where N_T is the number of target atoms per kg of detector⁶ and $f(v; v_E) = k$ is the velocity distribution of the mirror element, A^0 , with v being the velocity relative to the Earth, and v_E is the Earth velocity relative to the dark matter distribution. The lower velocity limit, $v_{\min}(E_R)$, is obtained from Eq.(5), while the upper limit, $v_{\max} = 1$, because of A^0 self interactions (as we will explain in a moment).

The velocity integral in Eq.(10),

$$I(E_R) = \int_{v_{\min}(E_R)}^{v_{\max}} \frac{f(v; v_E)}{k |\mathbf{v}|} d^3v \quad (11)$$

is standard (as it occurs also in the usual WIMP interpretation) and can easily be evaluated in terms of error functions assuming a Maxwellian dark matter distribution [29], $f(v; v_E) = k = (v_0^2)^{3/2} \exp[-(v + v_E)^2/v_0^2]$,

$$I(E_R) = \frac{1}{2v_0 y} [\text{erf}(x + y) - \text{erf}(x - y)] \quad (12)$$

⁶For detectors with more than one target element we must work out the event rate for each element separately and add them up to get the total event rate.

where

$$x = \frac{v_{min}(E_R)}{v_0}; y = \frac{v_E}{v_0} : \quad (13)$$

For standard non-interacting WIMPs, v_0 is expected to be in the (90% C.L.) range [30],

$$170 \text{ km/s} < v_0 < 270 \text{ km/s} : \quad (14)$$

In the case of a halo composed of H^0 ; $H^{\pm 0}$; heavier mirror elements and dust particles, there are important differences due to mirror particle self interactions. For example, assuming a number density of $n_{H^0} = 0.08 \text{ cm}^{-3}$ [c.f. Eq.(4)] the mean distance between H^0-H^0 collisions is $l = (n_{H^0} \sigma_{elastic})^{-1} = 0.03$ light years (using $\sigma_{elastic} = 3 \cdot 10^{16} \text{ cm}^2$). One effect of the self interactions is to locally thermally equilibrate the mirror particles in the halo. The H^0 (and other mirror particles) should be well described by a Maxwellian velocity distribution with no cutoff velocity. [H^0 do not escape from the halo because of their self interactions]. A temperature, T , common to all the mirror particles in the halo can be defined, where $T = M_{A^0} v_0^2/2$ (of course, T will depend on the spatial position). One effect of this is that v_0 should depend on M_{A^0} with

$$v_0(A^0) = v_0(H^0) \sqrt{\frac{M_{H^0}}{M_{A^0}}} : \quad (15)$$

Thus, knowledge of v_0 for H^0 will fix v_0 for the other elements. We will assume that the halo is dominated by H^0 (which is suggested by mirror BBN arguments [17]), with $v_0 = v_0(H^0)$ in the range, Eq.(14).

The Earth motion around the sun produces an annual modulation in y :

$$y = y_0 + y \cos!(t - t_0) \quad (16)$$

where $y_0 = hv_E/v_0$ and $y = v_E/v_0$ (for H^0 , $y_0 = 1.06$, $y = 0.07$). The parameter t_0 turns out to be June 2, and $! = 2\pi/T$ (with $T = 1$ year). Expanding $I(E_R)$ [Eq.12] into a Taylor series making the y dependence explicit, i.e. $I(E_R; y) = I(E_R)$:

$$I(E_R; y_0 + y \cos!(t - t_0)) = I(E_R; y_0) + y \cos!(t - t_0) \left. \frac{\partial I}{\partial y} \right|_{y=y_0} \quad (17)$$

and

$$\left. \frac{\partial I}{\partial y} \right|_{y=y_0} = \frac{I(E_R; y_0)}{y_0} + \frac{1}{v_0 y_0} e^{-(x-y_0)^2} + e^{-(x+y_0)^2} : \quad (18)$$

The net effect is an interaction rate

$$\frac{dR}{dE_R} = \frac{dR_0}{dE_R} + \frac{dR_1}{dE_R} \quad (19)$$

where

$$\begin{aligned} \frac{dR_0}{dE_R} &= \sum_{A^0} N_T n_{A^0} \frac{I(E_R; y_0)}{E_R^2} \\ \frac{dR_1}{dE_R} &= \sum_{A^0} N_T n_{A^0} \frac{y \cos!(t - t_0)}{E_R^2} \left. \frac{\partial I}{\partial y} \right|_{y=y_0} : \end{aligned} \quad (20)$$

Clearly, galactic mirror atom interactions will generate an annual modulation, $A \cos(\omega t + t_0)$, in the event rate coming from the $\frac{dR_1}{dE_R}$ component.

To compare these interaction rates with the experimental measurements, we must take into account the finite energy resolution and quenching factor. The quenching factor relates the detected energy (E_R) to the actual recoil energy (E),

$$E_R = q_A E \quad (21)$$

and for the DAMA experiment, q_{Na} ; q_I have been measured to be approximately $q_{Na} \approx 0.30$; $q_I \approx 0.09$ [1]. The energy resolution can be accommodated by convolving the rate with a Gaussian, with $\sigma_{res} = 0.16 E_R$ (from figure 3 of Ref.[31]).

The DAMA collaboration give their results in terms of the residual rate in the cumulative energy interval 2-6 keV, where they find that

$$A_{exp} = 0.019 \pm 0.003 \text{ cpd/keV} \quad (22)$$

This number should be compared with the theoretical expectation:

$$A_{th} = \frac{1}{4} \sum_{j=0}^{\infty} A_{th}^j \quad (23)$$

where

$$A_{th}^j = \sum_{A=Na, I} \frac{1}{E_j} \int_{E_j}^{E_j+E_0} \frac{q_A N_T n_{A^0}}{E_R^2} \frac{p}{2} \frac{\partial I}{\partial y} \bigg|_{y=Y_0} e^{-\frac{(E_R - E_R^0)^2}{2 \sigma_{res}^2}} dE_R^0 dE_R \quad (24)$$

with $E_j = 2.0 \text{ keV} + E_j$ ($j = 0; 1; 2; \dots$) and $E_0 = 1.0 \text{ keV}$.

We have numerically studied A_{th} . We find that the O^0 contribution to DAMA/NaI dominates over the He^0 (H^0) contribution provided that $\rho_{O^0=He^0} > 7 \cdot 10^4$ ($\rho_{O^0=H^0} > 4 \cdot 10^8$). The reason for this is of course clear: the actual threshold recoil energy is 6.7 keV for A^0 Na interactions⁷, which means that the v_{min} [from Eq.(5)] is:

$$\begin{aligned} v_{min}(H^0 \text{ Na}) &= 2830 \text{ km/s} \\ v_{min}(He^0 \text{ Na}) &= 795 \text{ km/s} \\ v_{min}(O^0 \text{ Na}) &= 290 \text{ km/s} \\ v_{min}(Fe^0 \text{ Na}) &= 166 \text{ km/s} \end{aligned} \quad (25)$$

⁷Numerically we find that mirror atom interactions with Na dominate over I for recoil energies above the 2 keV software threshold. This reason for this is clear: the threshold velocity is much lower for interactions with Na which is because a) Na is a much lighter element than I [c.f. Eq.(5)] and b) the quenching factor for Na is 0.3 (c.f. with 0.09 for I) which means that the actual recoil threshold energy is 6.7 keV for Na and 22 keV for I. Also note that the corrections due to the form factor, which were taken into account using the simple analytic expression, Eq.(7), are reasonably small ($\sim 5\%$) for $A^0 = O^0$ but larger ($\sim 30\%$) for $A^0 = Fe^0$.

Because $v_{\text{min}}(\text{H}^0 \text{ Na}) \ll v_0$, any H^0 contribution to the DAMA/NaI signal is expected to be very tiny and we will neglect it. The quantity $v_{\text{min}}(\text{He}^0 \text{ Na})$ is also quite high which suppresses the He^0 contribution relative to O^0 and Fe^0 .

Interpreting the annual modulation signal in terms of O^0 and Fe^0 , i.e. setting $A_{\text{th}} = A_{\text{exp}}$, we find numerically that:

$$\frac{A_{\text{O}^0}}{A_{\text{Fe}^0}} = \frac{0.10}{0.026} \pm 4.8^{+1.0}_{-1.3} \quad (26)$$

where the errors denote a 3 sigma allowed range (corresponding to $0.010 < A_{\text{exp}} < 0.028$). The best fit region will also be affected by systematic uncertainties in the quenching factors, form factors and astrophysical uncertainties [e.g. uncertainties in $v_0(\text{A}^0)$]. These uncertainties will increase the possible parameter range, however a detailed investigation of these effects we leave for the future.

Because of the different masses of the two components, O^0 and Fe^0 , their relative contributions can potentially be determined by the differential recoil energy spectrum, A^j . In figure 1 we examine the representative possibilities a) DAMA signal is dominated by O^0 [i.e. $A_{\text{O}^0} = 0.10$, $A_{\text{Fe}^0} = 0$ for $A \notin \text{O}^0$], b) DAMA signal is dominated by Fe^0 [i.e. $A_{\text{Fe}^0} = 0.026$, $A_{\text{O}^0} = 0$ for $A \notin \text{Fe}^0$]. The case where A_{th} is made up of approximately equal contributions from both O^0 and Fe^0 , corresponding to $A_{\text{O}^0} \approx 4 A_{\text{Fe}^0} = 0.05$ is also given. However, again we point out that a careful study of systematic uncertainties will be necessary before any definite conclusions can be made about the ratio of $A_{\text{O}^0} = A_{\text{Fe}^0}$.

Besides the annual modulation effect, DAMA/NaI has also measured the absolute event rate. This rate will contain the signal [$dR_0 = dE_R$, Eq.(20), convolved with a Gaussian to incorporate the detector resolution] plus any background contribution. An interesting point is that the cross section, Eq.(8), rises sharply ($\propto 1/E_R^2$) at low E_R , and this effect may show up in the data. [In any case, we should check that our absolute rate from the signal does not exceed the measured absolute rate]. In figure 2 we plot the absolute rate with parameters fixed by the annual modulation signal, Eq.(26). Also plotted is the measured rate obtained from Ref.[32]. Interestingly, the data does indeed show a sharp rise at low E_R which is compatible with the parameters suggested by the annual modulation effect. The shape of the measured rate at low E_R is nicely fitted by both O^0 and Fe^0 dark matter, but the normalization prefers O^0 over Fe^0 dark matter. However possible small systematic uncertainties such as calibration errors may be present: a 0.1-0.2 keVee calibration error would be enough to allow Fe^0 to fit the data at low E_R .

Implicit in our analysis is that the mirror atoms can reach the DAMA detector from all directions, without getting stopped in the Earth. The stopping distance of a mirror atom, A^0 (of energy $E^0 = \frac{1}{2} M_{\text{A}^0} v^2$) in ordinary matter (of atomic number density $n = \rho/M_{\text{A}}$) can easily be evaluated from :

$$\frac{dE^0}{dx} = \frac{Z}{M_{\text{A}}} E_R \frac{d}{dE_R} dE_R$$

$$= \frac{M_{A^0}^2 Z^2 Z^0 \ln \frac{E_R^{m \text{ ax}}}{E_R^{m \text{ in}}}}{M_A^2 E^0} \quad (27)$$

where $E_R^{m \text{ ax}}$ can be obtained from Eq.(5) and $E_R^{m \text{ in}} = 1 = (2r_0^2 M_A)$ (due to atomic screening). Explicitly, $\ln \frac{E_R^{m \text{ ax}}}{E_R^{m \text{ in}}} = 10$. Eq.(27) can be solved to give the energy of the mirror atom after travelling a distance x through ordinary matter:

$$E^0(x) = E^0(0) \exp\left(-\frac{x}{L}\right) \quad (28)$$

where L is the stopping distance:

$$L = \frac{M_A^2 M_{A^0}^4 v_i^4}{8 Z^2 Z^0 10} = \frac{10^8}{400 \text{ km} = \text{s}} \frac{v_i^4}{5 \text{ g} = \text{cm}^3} \frac{2}{Z^0} \text{ km} \quad (29)$$

where v_i is the initial velocity of the mirror atom. The stopping distance in earth for $H e^0$, O^0 and $F e^0$ can easily be obtained from the above equation, giving:

$$\begin{aligned} L(H e^0) &> 10^7 \text{ km for } j = 4 \cdot 10^9; v_i = v_{m \text{ in}}(H e^0) = 795 \text{ km} = \text{s}; \\ L(O^0) &> 5 \cdot 10^6 \text{ km for } j = 4 \cdot 10^9; v_i = v_{m \text{ in}}(O^0) = 290 \text{ km} = \text{s}; \\ L(F e^0) &> 3 \cdot 10^6 \text{ km for } j = 4 \cdot 10^9; v_i > 200 \text{ km} = \text{s}; \end{aligned} \quad (30)$$

Since $L(H e^0); L(O^0)$ are much larger than the Earth's diameter, the retarding effect of the Earth is relatively small and no large diurnal effect is expected (in agreement with DAMA observations[33]). Mirror iron, may lead to a possibly large diurnal effect. However, dark matter detection experiments depend on $j \cdot \frac{1}{A^0}$ while the stopping distance in earth, depends just on j . The significant uncertainty in the size of A^0 implies corresponding uncertainty in j and hence $L(A^0)$. It is therefore still possible for the DAMA/NaI signal to be dominated by the $F e^0$ component, without leading to any significant diurnal effect. Note that experiments with a lower threshold (and hence lower value of $v_{m \text{ in}}$) will have a much greater sensitivity to the diurnal effect, so this effect may show up in future experiments.

Let us now consider implications of this interpretation of the DAMA signal for other experiments. The CDM S/G e experiment[27] has searched for nuclear recoils due to WIM P-G e elastic scattering. This experiment has a threshold energy of 10 keV and the quenching factor is assumed (but not measured!) to be 1. This experiment finds just 4 events satisfying their cuts with $10 \text{ keV} < E < 20 \text{ keV}$ for their exposure of 10.6 kg-day. However because the target consists of the relatively heavy element, Ge, and the threshold is relatively high, 10 keV, the sensitivity of the CDM S experiment to light mirror elements, is completely negligible. Assuming $j \cdot j_0 = 0.10 = 4.8 \cdot 10^9$ (as suggested from the DAMA/NaI experiment, if O^0 dominates the rate), we find numerically that the number of O^0 induced events (above the 10 keV CDM S threshold) is much less than 1 for their exposure of 10.6 kg-day.

If there happens to be a significant $F e^0$ component, then this may potentially be constrained by CDM S/G e experiment. In the case where $F e^0$ dominates the DAMA/NaI experiment, then $j_j \approx \frac{R_{F e^0}}{R_{O^0}} = 4.8 \times 10^{-9}$. Numerically, we find that this implies 26 events in the $10 \text{ keV} < E < 20 \text{ keV}$ range for CDM S, for their 10.6 kg-day exposure (c.f. just 4 detected events). The low rate obtained by CDM S experiment suggests that $F e^0$ does not dominate over O^0 . However given possible experimental uncertainties, the case of $F e^0$ dominance is probably not completely excluded. For example, the quenching factor may turn out to be somewhat less than 1. For example, a value of 0.6 would reduce the expected number of events from 26 down to 5 events which is consistent with the data.

Clearly experiments with a lower threshold than DAMA/NaI might potentially provide more stringent constraints. The only experiment with a lower threshold than DAMA/NaI is the CRESST/Sapphire experiment [28]. That experiment uses 262 g sapphire crystals (Al_2O_3) as the target medium with a low detection threshold of $E_R (\text{threshold}) = 0.6 \text{ keV}$. These features make CRESST/Sapphire particularly sensitive to low mass dark matter particles such as $H e^0; O^0$ (and even $F e^0$). Unfortunately, the CRESST experiment does not have enough statistics to be sensitive to the annual modulation due to the Earth's motion around the sun, nevertheless the shape and normalization of the measured energy spectrum provide useful information⁸. We now study in detail the implications of mirror matter-type dark matter for this experiment.

In this experiment the quenching factor is assumed to be approximately equal to 1 (however, again this has not been specifically measured) [28]. As with the DAMA/NaI experiment, the recoil spectrum, Eq.(10), needs to be convolved with a Gaussian curve (with $\sigma_{res} = 0.4247 E_{res}$ ⁹) in order to take into account the finite energy resolution of the detector,

$$\frac{dR}{dE_R} = \int_0^Z \frac{1}{E_j} \frac{dR(E_R^0)}{dE_R^0} \frac{1}{\sqrt{2\pi}\sigma_{res}} e^{-\frac{(E_R - E_R^0)^2}{2\sigma_{res}^2}} dE_R^0 \quad (31)$$

The CRESST collaboration present their results in terms of the quantity,

$$C_j = \frac{1}{E_j} \int_{E_j}^{E_j + E} \frac{dR}{dE_R} dE_R \quad (32)$$

where $E_j = 0.6 \text{ keV} + E_j$ ($j = 0; 1; 2; \dots$) and $E = 0.2 \text{ keV}$. We have numerically studied C_j for various cases. In figure 3 we plot the expected value for C_j for the best fit values of $j_j \approx \frac{R_{A^0}}{R_{O^0}}$ assuming the DAMA/NaI rate is dominated by a) O^0 , b) $F e^0$ and c) 50-50 $O^0, F e^0$ mixture. Recall, these are the same three cases which were fitted

⁸Because of the low threshold, the CRESST experiment might be sensitive to the diurnal effect and this could even show up in the existing data.

⁹Note that $\sigma_{res} = \frac{E_{res}}{\sqrt{8 \ln 2}} = 0.4247 E_{res}$ implies a FWHM of E_{res} for the Gaussian curve, which is the CRESST prescription [28]. In Ref.[28], two values of E_{res} are discussed, $E_{res} = 0.2 \text{ keV}$ (from an internal calibration source) and $E_{res} = 0.5 \text{ keV}$ (from possible contamination with ^{55}Fe). In our numerical work we have used the former value (unless otherwise stated). Using $E_{res} = 0.5 \text{ keV}$ would lead to $j_j \approx \frac{R_{A^0}}{R_{O^0}}$ values smaller by about 20%.

to the DAMA/NaI annual modulation signal and were plotted in figure 1]. While the shape of the CRESST/Sapphire data (obtained from figure 10 of Ref.[28]) is reasonably consistent with the expected shape from A^0 interactions, the normalization is roughly a factor of 2 too high. This may be due to systematic uncertainties which we illustrate in figure 4. In this figure, the CRESST quenching factor is taken to be 0.7 instead of the assumed value of 1.0. (Similar results occur if there happens to be a small energy calibration uncertainty of ~ 0.2 keV). Figure 4 clearly demonstrates the rather nice fit of $O^0; F e^0$ dark matter to the shape and normalization of the CRESST data (after allowing for reasonable systematic uncertainties).

Given the rather nice fit of the shape and normalization of the CRESST data (within reasonable systematic uncertainties) to the expectations of $F e^0; O^0$ dark matter from the DAMA/NaI fit, it is clearly very tempting to suppose that the CRESST data may be mostly signal with very little background component. On the other hand, the CRESST collaboration [28] have argued that their data is most likely background because of the rate of coincidence events. This argument required the background to be due to single particle interactions and isotropic which it may not be.

Finally, note that the CRESST/Sapphire experiment is much more sensitive to $H^0; H e^0$ than the DAMA/NaI experiment. Assuming a pure $H e^0$ halo, i.e. $A^0 = 0$ for $A^0 \notin H e^0$, we find that the CRESST data suggest:

$$j j \frac{H e^0}{0.5} \lesssim 4 \times 10^9 \quad (33)$$

In this pure $H e^0$ halo limit, the (CRESST) value for $j j \frac{P}{H e^0}$, above, is not consistent with the value from DAMA/NaI [Eq.(26)]. Thus $H e^0$ cannot dominate the rate for DAMA or CRESST. This suggests that: $\rho_0 > 0.2 \rho_{H e^0}$ and/or $F e^0 > 0.04 \rho_{H e^0}$. Clearly this constraint is significant, but nevertheless, still allows $H e^0$ to be the dominant halo dark matter component¹⁰.

Assuming that DAMA and CRESST have detected galactic mirror matter-type dark matter, then this suggests an $j j$ value of around $10^8 - 10^9$. Previous work (see Ref.[13] and references therein) looking at various solar system implications of mirror matter has identified a similar but somewhat larger range for $j j$, Eq.(3). This information is summarized in figure 5. Also shown is the experimental bound [16, 15], $j j < 5 \times 10^7$ coming from recent orthopositronium lifetime measurements [34] and also the limit suggested from BBN [35].

Let us also mention that if $j j \lesssim 5 \times 10^9$, there will be interesting terrestrial effects of mirror matter. Fragments (of size R) of impacting mirror matter space bodies can remain on/near the Earth's surface provided that [36]

$$R < 5 \frac{j j}{5 \times 10^9} \text{ cm} \quad (34)$$

¹⁰Note that the CRESST/Sapphire experiment does not put significant limits on the H^0 component of the dark matter halo. Numerically, we find that $H e^0$ dominates over H^0 provided that $\rho_{H^0} < 15 \rho_{H e^0}$ which is not a very stringent condition.

Such fragments can potentially be detected and extracted with a centrifuge[36]. If mirror matter fragments become completely embedded within ordinary matter (which is necessarily the case for $\beta < 0$) then the fragments will thermally equilibrate with the ordinary matter environment. The observational effect of this is to cool the surrounding ordinary matter, as heat is transferred to the mirror body and radiated away into mirror photons[37]. Finally, even tiny solar system mirror dust particles can lead to observable effects. These particles impact with the Earth with velocity in the range $11 \text{ km/s} < v < 70 \text{ km/s}$ and can be detected in suitably designed surface experiments[38] such as the St. Petersburg experiment[39].

In conclusion, we have pointed out that the DAMA/NaI, CRESST/Sapphire and other dark matter experiments are sensitive to mirror matter-type dark matter. Furthermore, the annual modulation signal obtained by the DAMA/NaI experiment can be explained by mirror matter-type dark matter for $j \approx 5 \times 10^9$. This explanation of the DAMA signal is supported by DAMA's absolute rate measurement as well as by the size and shape of the CRESST data. Furthermore this explanation is not in conflict with CDM or any of the other dark matter experiments because of their higher thresholds. The value suggested by the DAMA/NaI experiment is consistent with the value obtained from various solar system anomalies including the Pioneer spacecraft anomaly, anomalous meteorite events and lack of small craters on the asteroid Eros. It is also consistent with standard BBN.

Acknowledgements: The author would like to thank Profs. R. Bernabei, R. Cerulli, F. Probst for patiently helping me understand some details regarding their experiments. The author also thanks R. Bernabei and R. Volkas for very valuable comments on a draft of this paper.

References

- [1] R. Bernabei et al. (DAMA Collaboration), Phys. Lett. B 389, 757 (1996); *ibid* B 424, 195 (1998); *ibid* B 450, 448 (1999); *ibid* B 480, 23 (2000); Eur. Phys. J C 23, 61 (2002); Phys. Rev. D 61, 023512 (1999); *ibid* D 66, 043503 (2002).
- [2] R. Bernabei et al. (DAMA Collaboration), Riv. Nuovo Cimento. 26, 1 (2003) [astro-ph/0307403].
- [3] R. Foot, H. Lew and R. R. Volkas, Phys. Lett. B 272, 67 (1991). The idea was earlier discussed, prior to the advent of the standard model, in: T. D. Lee and C. N. Yang, Phys. Rev. 104, 256 (1956); I. Kobzarev, L. Okun and I. Pomerenchuk, Sov. J. Nucl. Phys. 3, 837 (1966).
- [4] R. Foot, hep-ph/0207175; R. Foot, Acta Phys. Pol B 32, 2253 (2001) [astro-ph/0102294]; A. Yu. Ignatiev and R. R. Volkas, Talk given at the Australian Institute of Physics Congress, July 2002 [hep-ph/0306120]; Z. Silagadze, Acta

- Phys. Pol. B 32, 99 (2001) [hep-ph/0002255]; R. Foot, *Shadowlands: Quest for mirror matter in the Universe*, Universal Publishers, FL, 2002.
- [5] R. Foot, H. Lew and R. R. Volkas, *Mod. Phys. Lett. A* 7, 2567 (1992).
- [6] R. Foot, *Mod. Phys. Lett. A* 9, 169 (1994) [hep-ph/9402241]; R. Foot and R. R. Volkas, *Phys. Rev. D* 52, 6595 (1995) [hep-ph/9505359].
- [7] B. Holdom, *Phys. Lett. B* 166, 196 (1986).
- [8] R. Foot, A. Yu. Ignatiev and R. R. Volkas, *Phys. Lett. B* 503, 355 (2001) [astro-ph/0011156].
- [9] R. Foot and R. R. Volkas, *Phys. Lett. B* 517, 13 (2001) [hep-ph/0108051].
- [10] J. D. Anderson et al., *Phys. Rev. D* 65, 082004 (2002) [gr-qc/0104064].
- [11] R. Foot, *Acta Phys. Polon. B* 32, 3133 (2001) [hep-ph/0107132]; R. Foot and T. L. Yoon, *Acta Phys. Polon.* 33, 1979 (2002) [astro-ph/0203152].
- [12] M. Morawska-Horawska, A. Manechi, *Przegląd Geologiczny* 40, 335 (1995); J. A. Docobo, R. E. Spalding, Z. Cepelcha, F. Diaz-Fierros, V. Tamazian and Y. Onda, *Meteoritics & Planetary Science* 33, 57 (1998); A. O. Ikhovatorov, <http://olkhov.narod.ru/gr1997.htm>. The Jordan event, <http://www.jas.org.jp/mett.html>; N. V. Vasilyev, *Planet. Space Sci.* 46, 129 (1998) and references therein; P. W. Haines, R. J. F. Jenkins and S. P. Kelley, *Geology*, 29, 899 (2001).
- [13] R. Foot and S. Mitra, *Astroparticle Phys.* 19, 739 (2003) [astro-ph/0211067].
- [14] A. F. Cheng et al., *Science* 292, 484 (2001).
- [15] S. L. Glashow, *Phys. Lett. B* 167, 35 (1986); R. Foot and S. N. Gninenko, *Phys. Lett. B* 480, 171 (2000) [hep-ph/0003278].
- [16] R. Foot, astro-ph/0309330.
- [17] Z. Berezhiani, D. Comelli and F. L. Villante, *Phys. Lett. B* 503, 362 (2001) [hep-ph/0008105]; A. Yu. Ignatiev and R. R. Volkas, *Phys. Rev. D* 68 023518 (2003) [hep-ph/0304260]. For pioneering work, see also S. I. Blinnikov and M. Yu. Khlopov, *Sov. J. Nucl. Phys.* 36, 472 (1982); *Sov. Astron.* 27, 371 (1983).
- [18] D. N. Spergel et al. (WMAP Collaboration), *Ap. J. Suppl.* 148, 175 (2003) [astro-ph/0302209].
- [19] R. Foot and R. R. Volkas, *Phys. Rev. D* 68, 021304 (2003) [hep-ph/0304261].
- [20] C. A. Alcock et al. (MACHO Collaboration), *Astrophys. J.* 542, 281 (2000) [astro-ph/0001272].

- [21] Z. Silagadze, Phys. Atom. Nucl. 60, 272 (1997) [hep-ph/9503481]; S. Blinnikov, astro-ph/9801015; R. Foot, Phys. Lett. B 452, 83 (1999) [astro-ph/9902065].
- [22] R. Foot, A. Yu. Ignatiev and R. R. Volkas, Astropart. Phys. 17, 195 (2002) [astro-ph/0010502].
- [23] R. Foot, Phys. Lett. B 471, 191 (1999) [astro-ph/9908276]; Phys. Lett. B 505, 1 (2001) [astro-ph/0101055].
- [24] See e.g. D. C. B. Whittet, Dust in the galactic environment, IOP, Bristol 1992.
- [25] R. Foot and H. Lew, hep-ph/9411390, July 1994; Z. Berezhiani and R. N. Mohapatra, Phys. Rev. D 52, 6607 (1995) [hep-ph/9505385]; R. N. Mohapatra and V. L. Teplitz, Phys. Lett. B 462, 302 (1999) [astro-ph/9902085].
- [26] R. Foot, H. Lew and R. R. Volkas, JHEP 0007, 032 (2000) [hep-ph/0006027].
- [27] R. Abusaidi et al. (CDMS Collaboration), Phys. Rev. Lett. 84, 5699 (2000).
- [28] G. Angloher et al. (CREST Collaboration), Astroparticle Phys. 18, 43 (2002).
- [29] J. D. Lewin and P. F. Smith, Astroparticle Phys. 6, 87 (1996).
- [30] C. S. Kochanek, Astrophys. J. 457, 228 (1996).
- [31] R. Bemabei et al. (DAMA Collaboration), Eur. Phys. J. C 18, 283 (2000).
- [32] R. Bemabei et al. (DAMA Collaboration), Phys. Lett. B 480, 23 (2000).
- [33] R. Bemabei et al. (DAMA Collaboration), Il Nuovo Cimento A 112, 1541 (1999).
- [34] R. S. Vallery et al, Phys. Rev. Lett. 90, 203402 (2003).
- [35] E. Carlson and S. L. Glashow, Phys. Lett. B 193, 168 (1987).
- [36] S. Mitra and R. Foot, Phys. Lett. B 558, 9 (2003) [hep-ph/0301229].
- [37] R. Foot and S. Mitra, Phys. Lett. A 315, 178 (2003) [cond-mat/0306561].
- [38] R. Foot and S. Mitra, Phys. Rev. D 68 071901 (2003) [hep-ph/0306228].
- [39] E. M. Drobyshevski et al, Astronomical and Astrophysical Transactions, Vol. 22, 19 (2003) [astro-ph/0108231]; astro-ph/0305597.

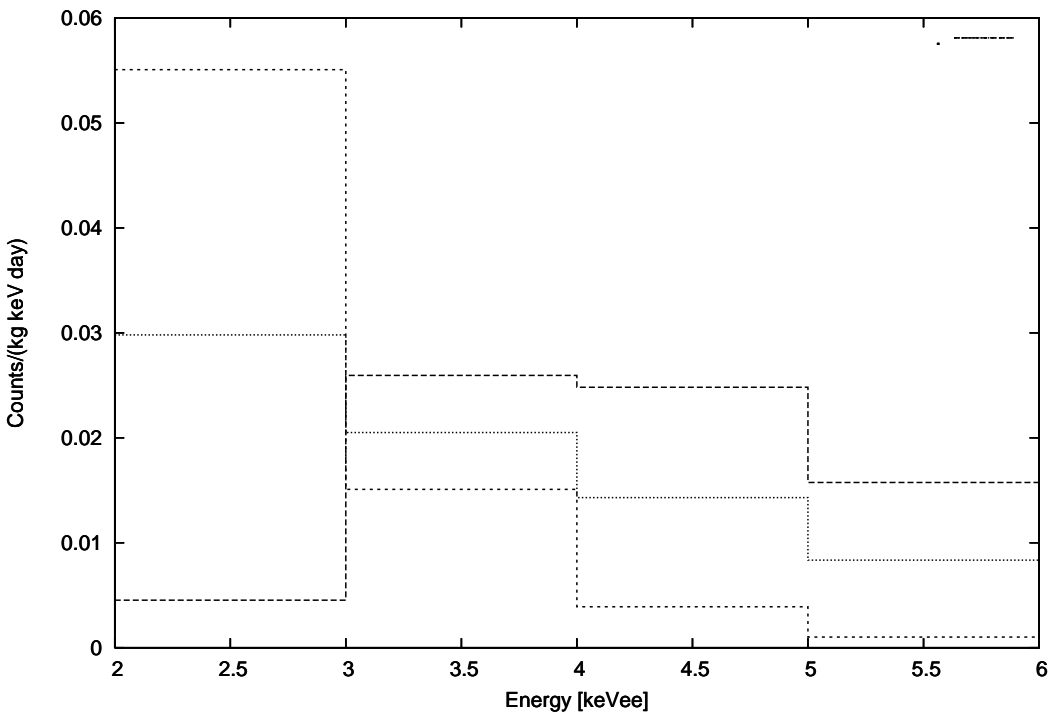


Figure 1: A_{th}^j (as defined in text) corresponding to the DAMA experiment for O^0 , F_{e^0} dark matter (for $v_0 = 230 \text{ km/s}$), with parameters $j = \frac{P_{O^0=0.10}}{P_{O^0=0.26}} = 4.8 \cdot 10^{-9}$, $A^0 = 0$ for $A^0 \notin O^0$ (short-dashed line), $b) \ j = \frac{P_{F_{e^0}=0.026}}{P_{F_{e^0}=0.26}} = 4.8 \cdot 10^{-9}$, $A^0 = 0$ for $A^0 \notin F_{e^0}$ (long-dashed line), $c) \ j = 4.8 \cdot 10^{-9}$ with $O^0 = 4 \cdot 10^{-9}$, $A^0 = 0.05$ (dotted line). In all three cases the differential rate in the 2-6 keV window agrees with the experimental value: $\frac{1}{4} \cdot P_{j=0}^3 \cdot A_{\text{th}}^j$, A_{exp} and the effect for $E_R > 6 \text{ keV}$ is negligible.

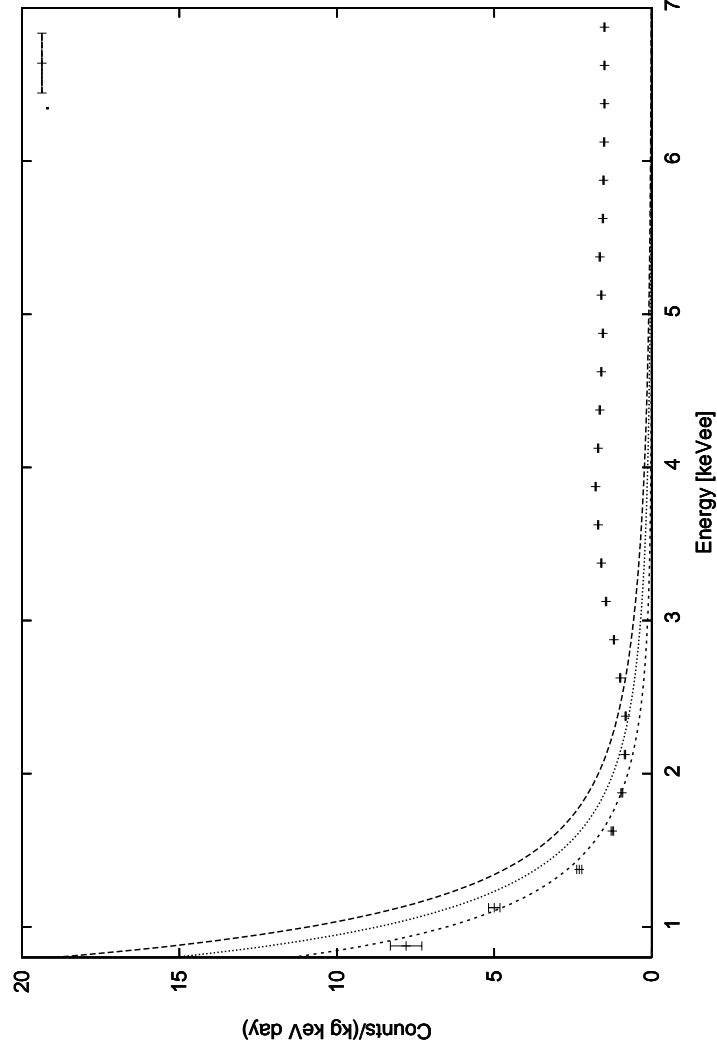


Figure 2: The absolute event rate for the DAMA/NaI experiment for $O^0; Fe^0$ dark matter (for $v_0 = 230$ km/s). The parameters are given by the fit to the DAMA/NaI annual modulation effect, where we take the same three representative cases as figure 1: a) $\frac{p}{j} \frac{O^0}{Fe^0} = 0.10 = 4.8 \times 10^{-9}$, $A^0 = 0$ for $A^0 \notin O^0$ (short-dashed line) b) $\frac{p}{j} \frac{Fe^0}{Fe^0} = 0.026 = 4.8 \times 10^{-9}$, $A^0 = 0$ for $A^0 \notin Fe^0$ (long-dashed line) and c) $\frac{p}{j} = 4.8 \times 10^{-9}$ with $\frac{O^0}{Fe^0} = 4$ $A^0 = 0.05$ (dotted line). Also shown is the DAMA/NaI data obtained from Ref.[32].

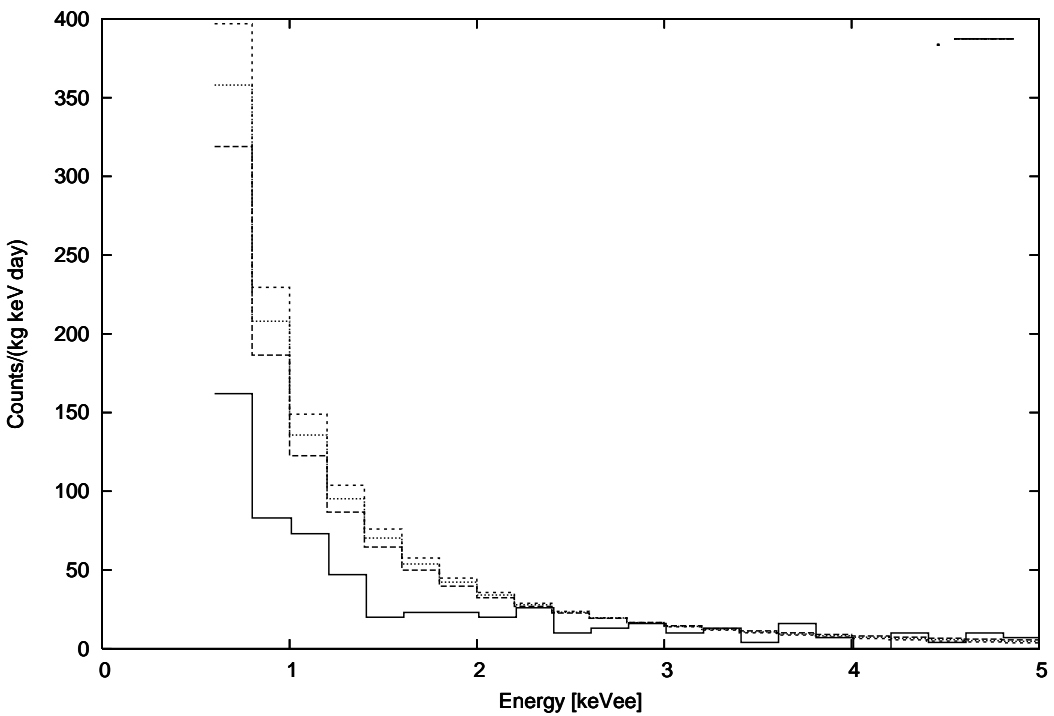


Figure 3: Expectation for the CRESST experiment for $v_0 = 230$ km/s and a) $\frac{P}{v_0=0.10} = 4.8 \cdot 10^9$ (short-dashed line), b) $\frac{P}{F_{e0}=0.026} = 4.8 \cdot 10^9$ (long-dashed line), c) $\frac{P}{v_0 = 4.8 \cdot 10^9}$ with $v_0 = 4.8 \cdot 10^9$ and $F_{e0} = 0.05$ (dotted line). Also shown (solid line) is the CRESST data obtained from figure 10 of Ref. [28]. Note that the statistical errors in the data are 15–30% for $E_R = \text{key} = 0.6$ –2.0 and $> 30\%$ for $E_R > 2.0$ keV.

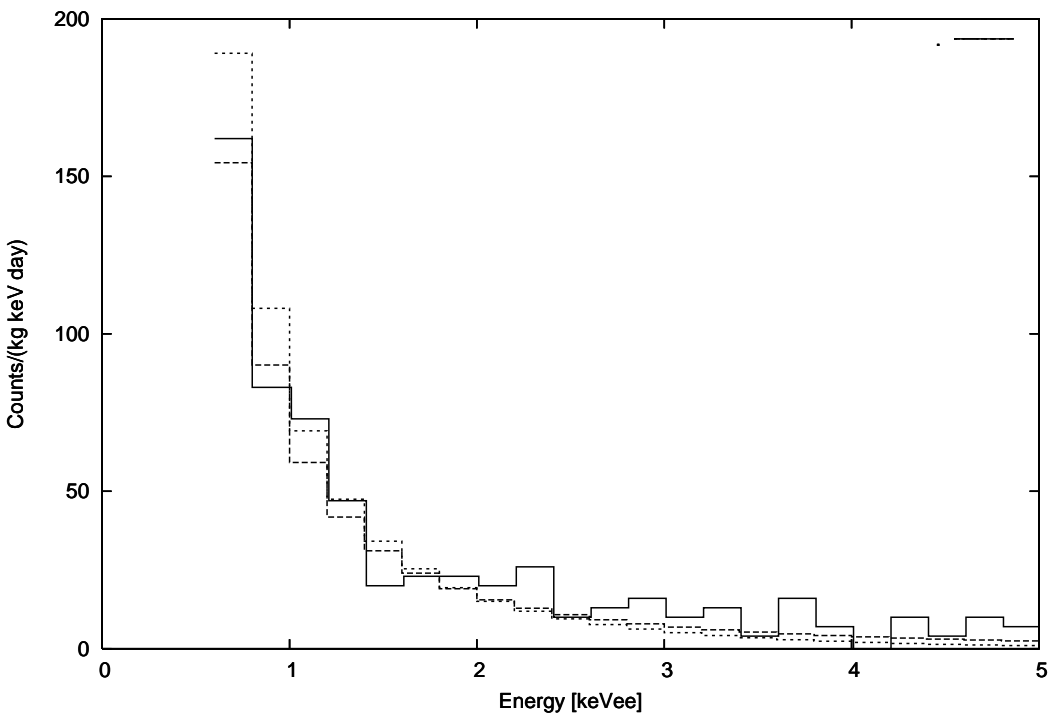


Figure 4: Expectation for the CRESST experiment for $\overline{\sigma_{\text{dark}}^{\text{ann}}}$ with $v_0 = 230 \text{ km/s}$ and a) $\overline{\sigma_{\text{dark}}^{\text{ann}}} = 4.0 \cdot 10^{-9}$ (short-dashed-line), b) $\overline{\sigma_{\text{dark}}^{\text{ann}}} = 4.0 \cdot 10^{-9}$ (long-dashed-line). In both cases, a CRESST quenching factor of $q = 0.7$ (instead of 1) has been assumed. Also shown (solid line) is the CRESST data.

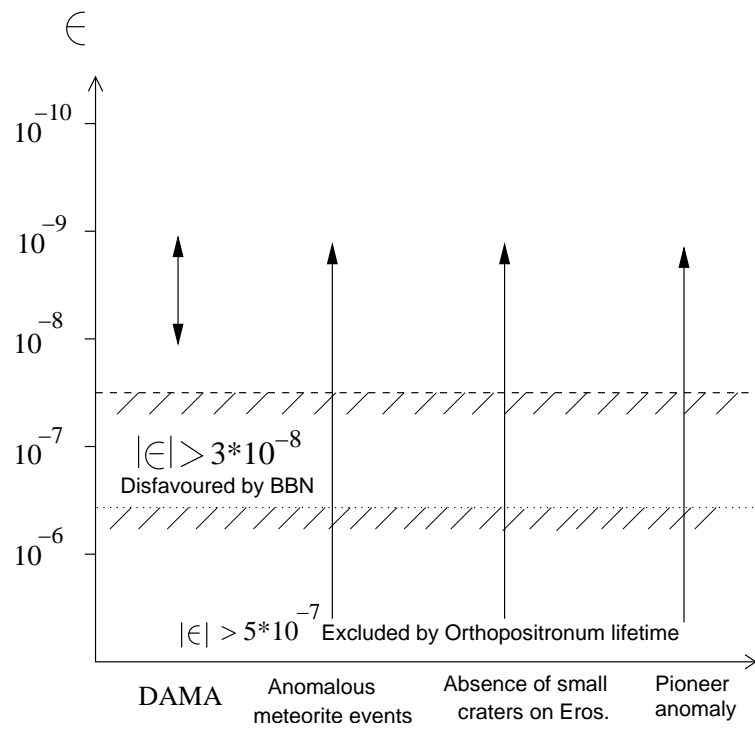


Figure 5: Favoured range of ϵ from various experiments/observations.